SERI/TP-252-2330
UC Category: 64
DE84013011

Open Cycle OTEC Thermal-Hydraulic Systems Analysis and Parametric Studies

Brian Parsons
Desikan Bharathan
Jay Althof

June 1984

To be presented at the
Oceans '84 Conference
Washington, D.C.
10 September 1984

Prepared under Task No. 4001.22
FTP No. 457-84

Solar Energy Research Institute
A Division of Midwest Research Institute

1617 Cole Boulevard
Golden, Colorado 80401

Prepared for the
U.S. Department of Energy
Contract No. DE-AC02-83CH10093

Printed in the United States of America
Available from:
National Technical Information Service
U.S. Department of Commerce
5285 Port Royal Road
Springfield, VA 22161
Price:
Microfiche A01
Printed Copy A02

OPEN CYCLE OTEC THERMAL-HYDRAULIC SYSTEMS ANALYSIS AND PARAMETRIC STUDIES

Brian Parsons, Desikan Bharathan, Jay Althof

Solar Energy Research Institute
1617 Cole Boulevard
Golden, Colorado 80401

Abstract

We have developed an analytic thermohydraulic systems model of the power cycle and seawater supply systems for an open cycle ocean thermal energy conversion (OTEC) plant that allows us ready examination of the effects of system and component operating points on plant size and parasitic power requirements. This paper presents the results of three parametric studies on the effects of system temperature distribution, plant gross electric capacity, and the allowable seawater velocity in the supply and discharge pipes. The paper also briefly discusses the assumptions and equations used in the model and the state-of-the-art component limitations. The model provides a useful tool for an OTEC plant designer to evaluate system trade-offs and define component interactions and performance.

Nomenclature

HTU	condenser height of a transfer unit
NTU	condenser number of transfer units
T_{cwi}	cold seawater condenser inlet temperature
T_{se}	evaporator steam temperature
T_{so}	turbine steam outlet temperature
T_{wwi}	warm seawater evaporator inlet temperature
T_{wwo}	warm seawater evaporator outlet temperature
ε_w	evaporator effectiveness

1. Introduction

1.1 Resource and Technology

The oceans contain a great amount of stored thermal potential energy. The temperature difference between the surface and deep water creates thermal gradients that can be turned into electricity. The conversion technology is similar to that used in conventional power plants. The sensible energy contained in the warm surface water is used to vaporize a working fluid that is then expanded through a turbine connected to an electric generator. A condenser maintains low pressure at the turbine exit using cold seawater as the energy sink.

Over a century ago, d'Arsonval [1] first suggested using ocean thermal gradients to generate power using a closed-cycle system. This system uses a secondary working fluid, such as ammonia, to drive a turbine. Surface heat exchangers evaporate and condense the working fluid while separating the working fluid from the seawater. Using a secondary working fluid allows the power cycle to operate at a higher pressure.

In 1930, George Claude [2], a student of d'Arsonval, proposed and demonstrated an alternative cycle, the open cycle, that uses steam evaporated directly from the seawater to power a turbine. Since the seawater temperature is less than the normal boiling point at atmospheric pressure, the power cycle pressure must be subatmospheric. Low pressure at the turbine exit may be maintained by a surface condenser, which has an added benefit of producing fresh water as a by-product, or by a direct-contact condenser in which the steam condenses directly on the cold seawater.

In 1979, Westinghouse Electric Corporation completed a comprehensive analysis of a 100-MW_e net floating, open cycle plant for the Department of Energy [3]. The analysis projected that floating plants in the range of 35-100 MW_e would be cost effective. The report identified several technical uncertainties and unknowns along with their potential for improving the plant's performance and economic viability. The largest potential cost impacts were associated with the evaporator, mist removal device, and condenser. Since that time, research at the Solar Energy Research Institute (SERI) and its contractors have addressed these and other important issues [4-12].

This paper summarizes a recent effort [10] that integrates the up-to-date developments in open-cycle OTEC components into an overall thermal-hydraulic systems analysis. The computer program developed, OTECSYS, allows a plant designer and a researcher to evaluate the impacts of component performance and design conditions on plant and component size and parasitic power requirements.

1.2 Open Cycle System Description

A block diagram of the basic open cycle system is presented in Fig. 1. Warm tropical seawater (~25°C) is pumped from near the ocean surface into an evacuated evaporator chamber where the pressure is lower than the corresponding saturation condition of the entering seawater. Flash evaporation results, cooling the seawater and converting a small portion of it (0.5%) to low-pressure steam.

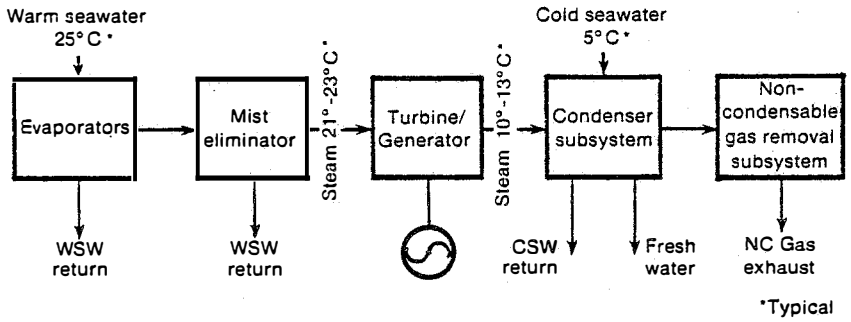

Fig. 1. Block Diagram of an Open Cycle OTEC System

The cooler seawater (~20°C) is then discharged back into the ocean. For some evaporator designs, the boiling process may entrain seawater in the steam, causing corrosion and erosion of the turbine blades. To mitigate this problem, a mist removal device may be required.

The steam expands through a turbine and a diffuser towards the condenser. A generator connected to the turbine produces the electric power, which also operates the seawater pumps and the exhaust compressors.

Cold seawater (~5°C) is pumped from depths of around 1000 m into the condenser to maintain the condenser pressure. Dissolved gases, present in the seawater, may come out of solution. To prevent an increase in pressure and loss in efficiency in the condenser, these gases, along with air leakage into the vacuum enclosure must be removed by an exhaust system.

2. Discussion of the Computer Model

A detailed description of the equations and procedures contained in the OTECSYS computer model is beyond the scope of this paper (see Parsons et al. [10]). However, a brief description follows. A main execution routine sets (or varies) the operating conditions and performance parameters of the plant. The overall system variables (determined by the main routine) are the generator gross power, the cold and warm seawater inlet temperatures, and the turbine inlet and outlet temperatures. Parameters for each component are also set and passed to the corresponding subroutine. The overall model is segmented using a subroutine for each component, making it easy to update component models as needed in the future.

2.1 Turbine

The first subroutine to be executed is the turbine model. Using specified turbine and generator efficiencies, the gross power, and inlet and outlet steam temperatures, we can compute the required steam mass flow rate. An input maximum tip speed and hub-to-tip ratio are used in an iterative process to find the inlet and outlet steam velocities, the turbine diameter, and speed. The turbines modeled in this study are similar to the large, low-pressure, last stage, axial machines used in conventional power plants.

2.2 Diffuser

The diffuser subroutine calculates the steam conditions at the condenser inlet based on a specified steam velocity and sizes the diffuser based on correlated conical axial diffuser data [13]. Diffuser exit conditions are found from a mass and energy balance and the turbine exit conditions. We can also specify a finite pressure drop between the diffuser and condenser through a vapor-passage pressure loss coefficient.

2.3 Evaporator

The evaporator subroutine determines the warm seawater flow rate from the steam temperature, water inlet temperature, and the evaporator effectiveness, defined as:

$$\varepsilon_w = (T_{wwi} - T_{wwo})/(T_{wwi} - T_{se}) .$$

The steam temperature is slightly higher than the turbine inlet temperature due to the pressure drop through a mist removal device. Pressure drop is calculated from an input pressure loss coefficient. (Typical values of this coefficient may be found in Bharathan and Penney [6].)

Evaporator effectiveness is a function of the evaporator geometry and operating conditions. Correlations for ε_w for a vertical spout geometry [5] are entered in the routine. The details and relative merits of this and other possible evaporator geometries are discussed in Bharathan et al. [4] and Penney et al. [11]. The warm seawater flow rate is then determined from a heat balance on the steam and warm seawater.

The second function of the routine is to estimate the planform area of the evaporator based on a calculated seawater flow rate. In addition, the amount of nitrogen and oxygen desorbed from the warm seawater is also computed from a specified fraction of the equilibrium gas release at the evaporator pressure.

2.4 Condenser

Currently a direct-contact condenser is modeled in the program. The routine is structured

to accept performance data for a variety of packings with a liquid distribution system. An initial cocurrent section, assumed to have a negligible vapor pressure drop, condenses most of the steam. This is followed by a countercurrent section that incurs an input pressure drop and further concentrates the inert gas and steam mixture ahead of the exhaust compressors.

Similar to the evaporator, the condenser subroutine has two main functions, namely, finding the cold seawater flow rate and sizing the unit. Specified operating conditions allow the number of transfer units (NTU) (related to the amount of steam condensed) to be calculated for each section. A desired contactor packing is selected by specifying the height of a transfer unit (HTU) (related to efficiency of the contactor) and the countercurrent vapor pressure drop. The overall height of the contacting device is HTU × NTU.

The cold seawater flow rate is found by multiplying the minimum theoretical flow required to reach desired design steam temperatures by an input design-to-minimum ratio. The area of the condenser is found from parameters that specify the liquid loading of the packing. As in the evaporator, the amount of dissolved gases released from the cold seawater is also computed.

2.5 Exhaust Compressors

The exhaust compressor subroutine calculates the amount of power required to remove the noncondensable gases and uncondensed steam from the condenser. The number of compressor stages is an input. The parasitic power required per stage is a function of gas temperature, flow rate, pressure ratio, and input motor and compressor efficiencies. The routine includes interstage coolers that lower the gas temperature after compression and reduce the flow rate by condensing some of the steam. Their performance is entered as a vapor pressure drop and an exit gas temperature. The volumetric capacity of each of the compressor stages is also calculated.

2.6 Seawater Flow System

The seawater flow system subroutine finds the pressure losses of the warm and cold seawater flow loops through the OTEC plant. The inlet and discharge pipe lengths along with the pipe roughness are entered with either a specified pipe diameter or a desired seawater velocity in the pipe. The friction factor is calculated based on the roughness and fluid Reynolds number using the design formula for turbulent friction by Colebrook [14]. The routine also evaluates pressure losses caused by the pipe intake and discharge, bends, the heat exchanger, and seawater density differences.

2.7 Seawater Pumps

The seawater pump subroutine finds the parasitic power required to pump the warm and cold seawater through the plant given the previously calculated flow rate and pressure loss. The pump efficiency corresponds to typical low head, high flow, commercially available equipment. The program uses curve fits for a particular family of axial pumps to determine the pump diameter and rotational speed.

3. Results of Parametric Studies

We used this computer model to study the effects of varying the temperature distribution through the system for a 5-MW_e plant, the gross electric generating capacity of the plant, and the design water velocity in the seawater pipes. We found these parameters to have major impacts on the plant performance and net power production. Sample results included below illustrate how the model can be used in evaluating open-cycle OTEC plant designs.

3.1 System Temperature Distribution

For typical seawater resource temperatures of 25°C and 5°C, the 20°C available temperature differential can be apportioned through the system in any fashion. Choice of the system temperature distribution depends on the design criteria and the performance of each of the components. In this study, we determined the effects of the system temperature distribution on the net power production and component sizes for a 5-MW_e plant. We varied the turbine inlet and outlet temperatures and determined the evaporator outlet and the condenser inlet steam temperatures by specifying pressure drop parameters. Table 1 lists the important specified characteristics of the plant under study.

The variation in the fraction of net-to-gross power for the 5-MW_e plant is plotted in Fig. 2. The maximum net power fraction of nearly 75% occurs at a turbine inlet temperature of 20°C and a turbine outlet temperature of 12°C. This fraction does not change appreciably for up to 2°C changes in these temperatures.

Figure 3 shows the breakdown of the parasitic power into exhaust compressor and warm and cold seawater pump requirements. The cold water pump consumes the most parasitic power with 12%-15% of gross being typical. The changes in parasitic power caused by varied system temperature distribution are readily explained by examining the trends in the flow requirements of steam, cold seawater, and warm seawater as shown in Figs. 4, 5, and 6. For the fixed gross power of 5 MW_e, the product of the steam mass flow rate and enthalpy drop through the turbine must remain constant. With the enthalpy drop being nominally proportional to the steam temperature difference across the turbine, the steam mass flow rate varies inversely proportional to the turbine temperature drop as shown in Fig. 4.

With this in mind the trends in cold seawater flow rate shown in Fig. 5 can also be explained. Lowering the turbine inlet steam temperature at a constant turbine steam outlet temperature results in larger steam mass flow rates. Since the driving

TABLE 1

Characteristics of the Plant Examined in the System Temperature Distribution Study

Characteristics	Unit of Measure
Seawater resource	
warm seawater inlet temperature	
cold seawater inlet temperature	
Turbine	
gross power 5 MWe	
turbine total-to-static efficiency	0.81
generator efficiency	1.0
number of turbines	1
maximum tip speed	450 m/s
Diffuser	
exit steam velocity	60 m/s
Evaporator	
effectiveness	0.911
seawater velocity in the spout	2 m/s
mist removal steam velocity	30 m/s
mist removal pressure loss coefficient	10
evaporator-turbine pressure coefficient loss	0
actual/equilibrium gas release	0.9
atmospheric air leak rate	0 kg/s
Direct contact condenser	
supply pipe seawater velocities	2 m/s
inlet steam velocities	30 m/s
design/ideal seawater flows	1.2
countercurrent vapor pressure drop	200 Pa
outlet gas temperature elevation	1°C
height of transfer units	0.3 m
actual/equilibrium gas release	0.8
atmospheric air leak rate	0 kg/s
diffuser-condenser pressure coefficient loss	0
Condenser exhaust compressor train	
number of compressors	4
compressor efficiency	0.8
Seawater distribution system	
number of pipes per seawater loop	1
warm seawater inlet pipe length	500 m
cold seawater inlet pipe length	2750 m
warm and cold discharge pipe length	620 m
pipe seawater velocities	2.0 m/s
pipe roughness	46×10^{-6} m
number of 45° bends in the inlet discharge and pipe	10
evaporator spout length	2.7 m
condenser supply pipe length + contactor height	1.0 m
Seawater pumps	
number of pumps per seawater loop	1
pump efficiency	0.36

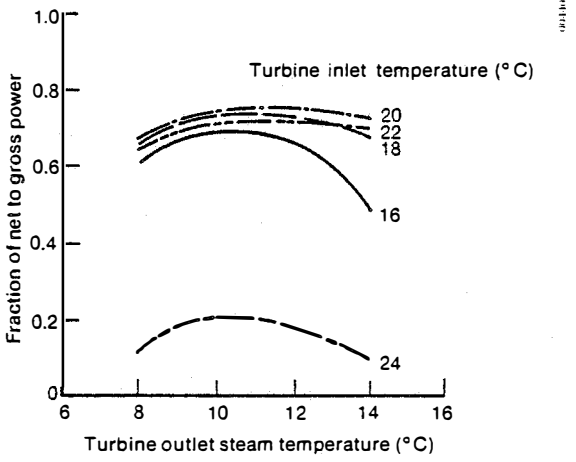

Fig. 2. Variation of Net Power Fraction with Turbine Inlet and Outlet Steam Temperatures for a 5-MW_e Shore-Based System

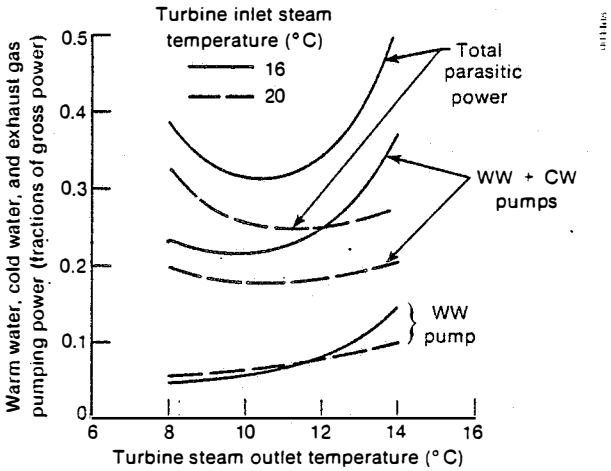

Fig. 3. Breakdown of Pumping Power for Warm Water, Cold Water, and Exhaust Gas with Turbine Inlet and Outlet Steam Temperatures for a 5-MW_e Shore-Based System

potential for condensation ($T_{so} - T_{cwi}$) is constant in this case, the required cold seawater flow also increases. At constant turbine inlet temperature the benefits of reduced steam flow rate caused by lowering the turbine outlet temperature are offset by the reduced driving force for condensation at outlet temperatures less than 11°C. However, for lower turbine inlet temperatures (16°-18°C) the increase in steam flow to be condensed as the turbine inlet and outlet temperatures approach each other overwhelms the effect of increased condensation driving potential. Therefore, for low turbine inlet temperatures the cold seawater flow rate exhibits a minimum value over the temperature ranges examined. Similar trends are indicated in Fig. 6 for the variation in warm seawater flow rate with changes in the system temperature distribution.

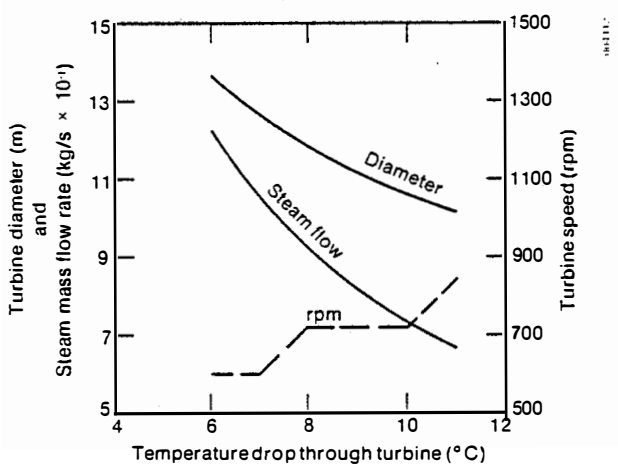

Fig. 4. Variations of Turbine Parameters with Turbine Temperature Drop for a 5-MW_e Shore-Based System

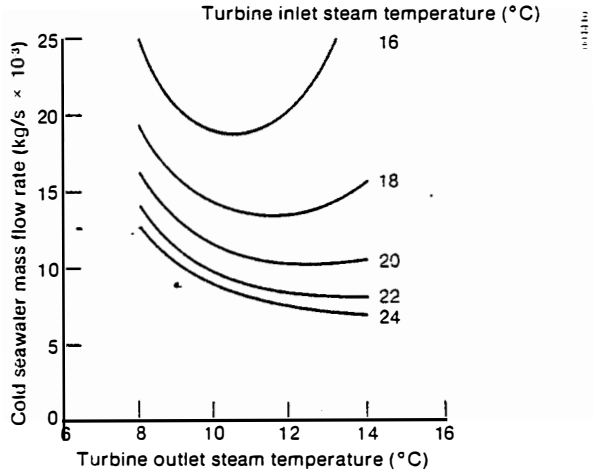

Fig. 5. Variation of Cold Seawater Flow Rate with Turbine Inlet and Outlet Steam Temperatures for a 5-MW_e Shore-Based System

The parasitic power required to circulate the seawater through the plant is proportional to the seawater flow rate. A secondary effect here is that the head loss decreases slightly with increasing flow rate since the pipe diameter gets larger (the water velocity is held constant). These factors lead to the results presented in Fig. 3 for warm and cold seawater parasitic power requirements.

The parasitic power required to exhaust the noncondensable gases from the condenser is related to the amount of gases released from the seawater, which are proportional to the water flow rates. The secondary effect is that the amount of gases released is also a function of the heat exchanger pressure. The lower the steam temperature (and the corresponding saturation pressure), the larger is

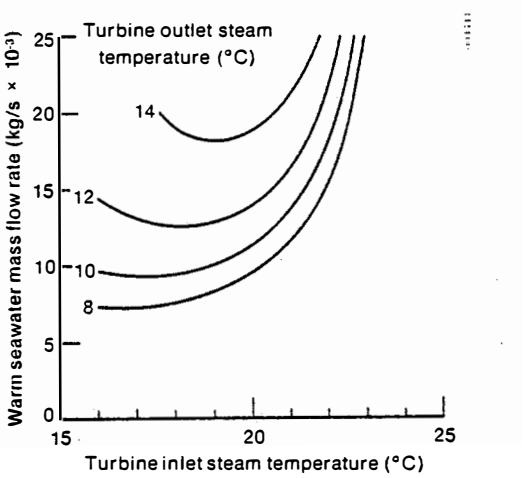

Fig. 6. Variation of Warm Seawater Flow Rate with Turbine Inlet and Outlet Steam Temperatures for a 5-MW_e Shore-Based System

the gas release per kilogram of seawater. These two effects combine to result in exhaust power requirements as shown in Fig. 3.

The system temperature distribution also influences component and plant sizes. Since size provides a measure for the capital cost, these sizes also influence the choice of the system temperature distribution. Figure 7 presents the variation in the combined area of the evaporator and condenser at the barometric level of the plant. This planform area is nominally proportional to the sum of the warm and cold water flow rates, and reaches a minimum at a turbine inlet temperature of around 19°C and an outlet temperature of 9°C. As turbine outlet temperatures decrease below 9°C, the required planform area increases mainly because of an increase in cold water flow rate (omitted from the figure for clarity).

The diameter of the 5-MW_e turbine also changes with the system temperature distribution (Fig. 4). Increased steam flow rate results in larger turbine flow areas; however, the area is related to the steam volumetric flow at turbine exit. An increase in the turbine outlet temperature results in a decrease in steam specific volume and, hence, the turbine diameter. A smaller turbine rotates at higher speeds. The step-changes in speed result from choosing rpms in multiples of 60 Hz to allow simpler coupling between the turbine and generator.

3.2 Plant Generating Capacity

Westinghouse suggested that a considerable economy of scale is inherent in the design of open cycle OTEC plants. Their 1979 report [3] predicted that by increasing the plant capacity from 10 to 50 MW_e, the cost of produced electricity decreases by 40%. A study examining the effects of varying plant size on net-to-gross power fraction and the

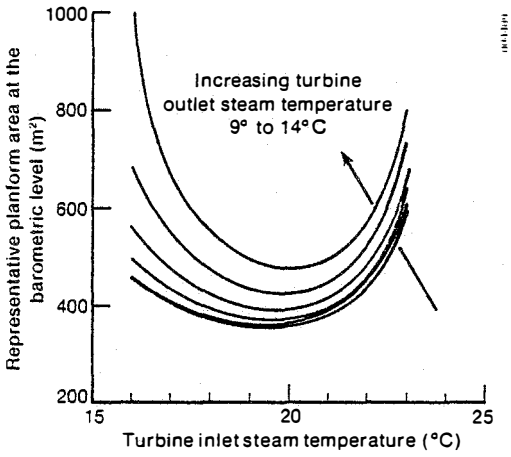

Fig. 7. Variation of a Representative Planform Area of the Heat Exchangers at the Barometric Level with Turbine Inlet and Outlet Steam Temperatures for a 5-MW_e Shore-Based System

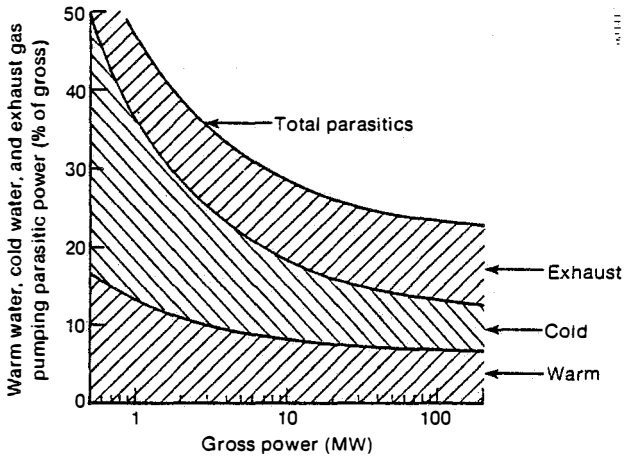

Fig. 8. Variation and Breakdown of Parasitic Power in the Plant Gross Capacity at Maximum Net Power Fraction

size of several key components was undertaken to illustrate the underlying causes for this cost reduction.

First, preliminary runs were made to ensure that the plant capacity does not alter the turbine inlet and outlet temperatures corresponding to a maximum gross-to-net power fraction provided all other design constraints are held constant. This study on the plant capacity used design conditions similar to those listed in Table 1. The study also included air leakage into the systems at a rate of nominally 10% in excess of the dissolved gas evolution and vapor-passage pressure losses through use of corresponding pressure loss coefficients. Turbine inlet and outlet temperatures of 20°C and 12°C were used.

Figure 8 illustrates the increase in net-to-gross power fraction as the plant capacity increases. For plants of less than 1 MW_e capacity, the seawater pumps consume a large fraction of the gross power due to smaller water pipe diameters and increased frictional losses. The net power fraction is less than 50%. As plant capacity increases, the net power fraction increases to about 75% at 100 MW_e capacity.

The condenser exhaust removal compressors consume a relatively constant fraction (10%) of the gross power independent of plant capacity. Consequently, the increase in net power fraction at larger plant sizes is a result of increased seawater pipe diameters. As evident from these dicussions, the net power fraction at any plant size can be increased by lowering the seawater velocities.

Figure 9 shows the variation of seawater intake pipe diameters with the plant size (equivalent to using single warm and cold water pipes at a water velocity of 2 m/s). Limiting the pipe diameter to a currently available maximum of 3 m will yield a gross capacity of 5 MW_e. Larger gross power may be achieved through the use of multiple

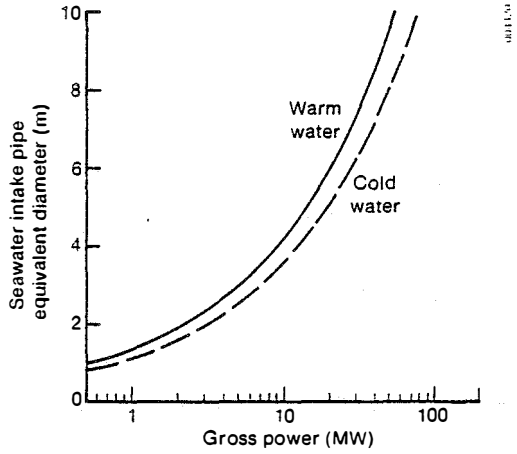

Fig. 9. Variations of Equivalent Seawater Pipe Diameters with Plant Gross Capacity at Maximum Net Power Fraction

pipes; but this would decrease the net power fraction below the values shown in Fig. 8.

Another component limiting the capacity of a near term practicality of the Claude open cycle OTEC plant is the turbine. The turbine diameter for plants with a single turbine is plotted as a function of gross electric capacity in Fig. 10. Low pressure turbines, which are used as the last stage in existing conventional power plants, have a maximum diameter of 4-5 m. Reputable turbine manufacturers have indicated that this hardware could easily be adapted to open cycle plants with a lead time of around two years [15]. A turbine diameter of 5 m corresponds to a gross electric capacity of about 2 MW_e. Use of multiple turbines would not alter the projected plant performance with the exception of increasing the vapor pressure losses caused by more complex steam routing.

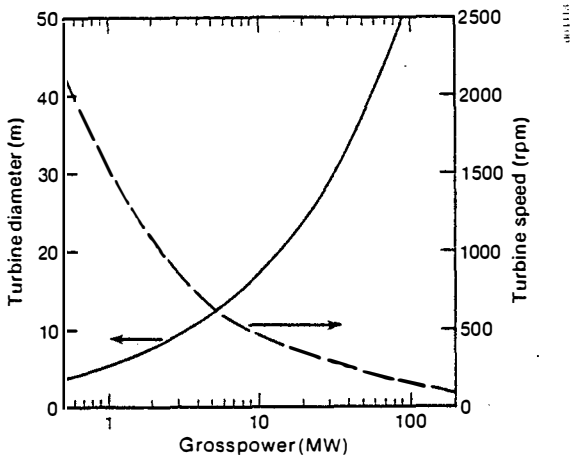

Fig. 10. Variations of Turbine Spaced and Diameter with Plant Gross Capacity at Maximum Net Power Fraction

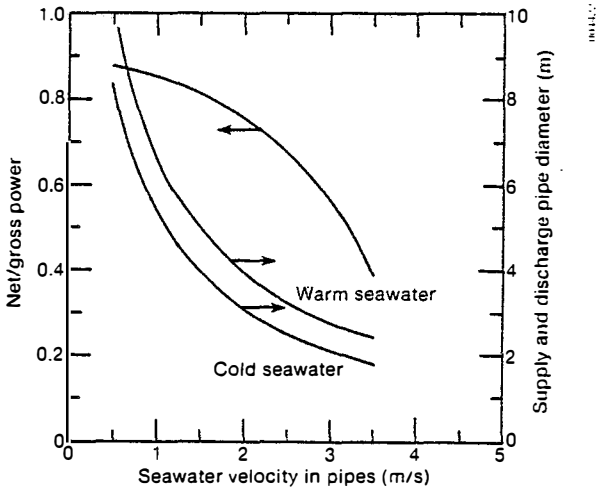

Fig. 11. Variations of Net Power Fraction and Seawater Pipe Diameters with Seawater Intake Velocity for a 5-MW_e Shore-Based System

Most other power cycle components are either off-the-shelf items or do not require any special manufacturing development. The evaporator and the condenser are modular components and their sizes can be increased in proportion to the required capacity. Defining a reliable leak rate into the vacuum chambers is an issue yet to be resolved concerning the heat exchangers. Other research issues such as the amount and effects of seawater entrainment in the steam, condenser performance, and reliability, etc., need also to be resolved, but these do not depend on the plant capacity.

3.3 Seawater Velocity in the Supply and Discharge Pipes

The head loss in the seawater pipes has a large influence on the net power fraction of the plant. Since these pipes are major cost items, the choice between reducing the pipe diameter (and increasing the seawater velocity and parasitic pumping power) to lower capital cost and increasing diameter to produce more net power depends on economic tradeoffs. However, it is instructive for us to examine the changes in net power fraction as a function of the pipe diameter. Parametric runs were performed to examine this effect for a 5-MW_e plant (see Table 1) by varying seawater velocity in the pipes from 0.5 to 3.5 m/s. Again, irrespective of the seawater velocity, the maximum net power fraction occurred at turbine inlet and outlet temperatures of 20°C and 12°C, respectively, in this study.

Fixing the plant gross capacity at 5 MW_e fixes the warm and cold seawater flow rates. Therefore, the pipe diameter is inversely proportional to the square root of the seawater velocity as shown in Fig. 11. The water head losses, being proportional to the square of the seawater velocity, drastically reduce the net power fraction as the velocity increases. Increasing the seawater velocity from 2 to 3.5 m/s decreases the warm and cold seawater pipe diameters by around 25%, yet the net power fraction is reduced from 75% to less than 40%.

4. Summary and Future Efforts

A useful and flexible systems analysis program has been developed for evaluating the performance of Claude open cycle OTEC plants. Each component in the power and hydraulic systems is modeled as a separate component, allowing simple integration of alternative component designs in the overall system. The components currently programmed reflect off-the-shelf technology for components, such as seawater pumps, exhaust compressors, generators, and water distribution. Models of components specific to the technology or that operate at conditions uncommon to general engineering practice, such as the evaporator, condenser, mist eliminator, and turbine are based on recent data from research results and projections. The developed program offers a unique and valuable tool to a designer in defining plant operating conditions, power requirements, and component sizes.

We performed several parametric studies using the model to examine the effects of the system temperature distribution, plant gross electric capacity, and seawater velocity in the flow pipes. Results indicate that for warm and cold seawater inlet temperatures of 25°C and 5°C, respectively, the maximum net-to-gross power ratio occurs at a turbine inlet steam temperature of around 20°C and an outlet temperature of nearly 12°C. This maximum net power fraction increases with increasing capacity of the plant due to pumping losses, which vary with pipe diameter, and decreasing seawater velocity in the pipes.

Future work pursued as part of a systems analysis integration effort by SERI, Argonne National Laboratory, and the Applied Physics Laboratory will provide a comparative evaluation for

competing OTEC technologies. Specific improvements for the open cycle analysis will include additional component model options (e.g., surface condensers), component costs and plant economics, and the capability to predict off-design plant performance.

5. Acknowledgment

The authors would like to express their gratitude to the U.S. Department of Energy, Ocean Energy Technology Division, for their support in carrying out this work.

6. References

1. D'Arsonval, Arsene, "Utilisation des forces natuelles: Avenir de L'electricite," La Revue Scientitique, 17 Sept 1881, pp. 370-372.

2. Claude, Georges, "Power from the Tropical Seas," Mechanical Engineering, Vol. 52, No. 12, December 1930, pp. 1039-1044.

3. Westinghouse Electric Corporation, 100 MW$_e$ OTEC Alternate Power Systems, U.S. DOE contract no. EG-77-C-05-1473, Vol. 1, March 1979.

4. Bharathan, D., Kreith, F., and Owens, W. L., "An Overview of Heat and Mass Transfer in Open-Cycle OTEC Systems," ASME/JSME Thermal Engineering Joint Conference Proceedings, Y. Mori and W. J. Wang, eds., Vol. 2, pp. 301-314, 1983.

5. Bharathan, D., and Penney, T., "Flash Evaporation from Falling Turbulent Jets," ASME/JSME Thermal Engineering Joint Conference Proceedings, Y. Mori and W. J. Wang, eds., Vol. 2, pp. 341-353, 1983.

6. Bharathan, D., and Penney, T., Mist Eliminators for Freshwater Production from Open-Cycle OTEC Systems, SERI/TR-252-1991, Golden, CO: Solar Energy Research Institute, December 1983.

7. Wassel, A. T., Bugby, D. C., Mills, A. F., and Farr, J. L., Jr., "Design Methodology for Direct-Contact Falling Film Evaporators and Condensers for Open Cycle Ocean Thermal Energy Conversion," SAI-083-83R-001, El Segundo, CA: Science Applications Inc., February 1982.

8. Bharathan, D., Olson, D. A., Green, H. J., and Johnson, D. M., "Measured Performance of Direct-Contact Jet Condensers," SERI/TP-252-1437, Golden, CO: Solar Energy Research Institute, January 1982.

9. Sam, R. G., and Patel, B. R., "Open Cycle Ocean Thermal Energy Conversion Evaporator/Condenser Test Program--Data Report," TN-340, Hanover, NH: Creare Research and Development, Inc., October 1982.

10. Parsons, B. P., Bharathan, D., and Althof, J. A., Thermodynamic Systems Analysis of Open-Cycle Ocean Thermal Energy Conversion, SERI/TR-252-2234, Golden, CO: Solar Energy Research Institute, forthcoming.

11. Penney, T., Bharathan, D., Althof, J., and Parsons, B., "Small-Scale, Shore-Based, Open-Cycle Ocean Thermal Energy Conversion Systems--A Design Case Study for an Integrated Research Facility," SERI/TP-252-2331, Golden, CO: Solar Energy Research Institute, forthcoming.

12. Bharathan, D. and Althof, J., "An Experimental Study of Steam Condensation on Water in Counter-current Flow in Presence of Inert Gases," SERI/TP-252-2332, Golden, CO: Solar Energy Research Institute, forthcoming.

13. Balje, O. E., Turbomachines, A Guide To Design, Selection, and Theory, New York: John-Wiley and Sons, 1981.

14. Colebrook, C. F., "Turbulent Flow in Pipes, with Particular Reference to the Transition Between Smooth and Rough Pipe Laws," J. Inst. Civ. Eng. Lond., Vol. 11, 1938-39, pp. 133-156.

15. Penney, T., Unpublished Letter Report from A. T. Wassel, Hermosa Beach, CA: Science Applications, Inc., 14 July 1983.